

See discussions, stats, and author profiles for this publication at: <https://www.researchgate.net/publication/269176031>

Solvation of a Cellulose Microfibril in Imidazolium Acetate Ionic Liquids: Effect of a Co-Solvent.

ARTICLE *in* THE JOURNAL OF PHYSICAL CHEMISTRY B · DECEMBER 2014

Impact Factor: 3.3 · DOI: 10.1021/jp508113a · Source: PubMed

CITATIONS

3

READS

101

8 AUTHORS, INCLUDING:



M. Göktug Ahunbay
Istanbul Technical University
29 PUBLICATIONS 340 CITATIONS

[SEE PROFILE](#)



Serife Birgül Tantekin-Ersolmaz
Istanbul Technical University
23 PUBLICATIONS 281 CITATIONS

[SEE PROFILE](#)



Margarida F Costa Gomes
French National Centre for Scientific Research
192 PUBLICATIONS 3,301 CITATIONS

[SEE PROFILE](#)



Agílio A H Pádua
Université Blaise Pascal - Clermont-Ferrand II
237 PUBLICATIONS 6,083 CITATIONS

[SEE PROFILE](#)

Solvation of a Cellulose Microfibril in Imidazolium Acetate Ionic Liquids: Effect of a Cosolvent

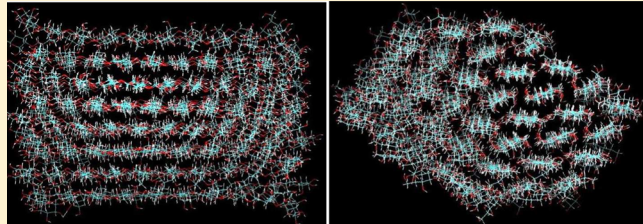
Sadiye Velioglu,[‡] Xun Yao,[†] Julien Devémy,[†] M. Goktug Ahunbay,[‡] S. Birgul Tantekin-Ersolmaz,[‡] Alain Dequidt,[†] Margarida F. Costa Gomes,[†] and Agílio A. H. Pádua^{*,†}

[†]Institut de Chimie de Clermont-Ferrand, Université Blaise Pascal & CNRS, 24 Avenue des Landais, 63171 Aubière, France

[‡]Istanbul Technical University, Department of Chemical Engineering, Maslak, 34469 Istanbul, Turkey

Supporting Information

ABSTRACT: The solvation and the onset of dissolution of a cellulose I_β microcrystal in ionic liquid media are studied by molecular simulation. Ionic liquids can dissolve large amounts of cellulose, which can later be regenerated from solution, but their high viscosity is an inconvenience. Hydrogen bonding between the anion of the ionic liquid and cellulose is the main aspect determining dissolution. Here we try to elucidate the role of a molecular cosolvent, dimethyl sulfoxide (DMSO), which is an aprotic polar compound, in the system composed of cellulose and the ionic liquid 1-butyl-3-methylimidazolium acetate. We calculated quantities related to specific interactions (mainly hydrogen bonds), conformations, and the structure of local solvation environments, both for a solvated oligomer chain of cellulose and for a model microfibril composed of 36 chains in the I_β crystal structure. We compare two solvent systems: the pure ionic liquid and a mixed solvent with an equimolar composition in ionic liquid and DMSO. All entities are represented by detailed all-atom, fully flexible force fields. The main conclusions are that DMSO behaves as an “innocent” cosolvent, lowering the viscosity and accelerating mass transport in the system, but without interacting specifically with cellulose or disrupting the interactions between cellulose with the anions of the ionic liquid. An understanding of solvation in mixed solvents composed of ionic liquids and molecular compounds can enable the design of high-performance media for the use of biomass materials.



INTRODUCTION

Cellulose¹ is the most abundant biorenewable resource, outstanding for its thermal and chemical stability combined with biocompatibility and biodegradability. Cellulosic biomass products have major applications in the fiber, paper, membrane, polymer, paint, and pharmaceutical industries. The micro-crystalline structure of the native cellulose I structure is recalcitrant to enzymatic hydrolysis, although other structures, such as amorphous cellulose, cellulose II, and cellulose III, are less recalcitrant. In the cellulose I lattice, chains are aligned parallel to each other, with strong hydrogen bonding and van der Waals (vdW) forces that lead to compact and highly ordered microfibrils. This compactness hinders dissolution in many solvents, forcing the use of derivatization or harsh and environmentally unfriendly chemicals. With increasing regulations restricting the use of the current solvents, the need to replace them is becoming more important.

Among the potential new solvents,² ionic liquids (ILs)³ are effective dissolving cellulose⁴ and lignocellulosic biomass under mild conditions. The physical and chemical properties of these liquid materials can be fine-tuned through judicious selection of their cation and anion moieties. ILs can thus be made to dissolve a wide range of compounds and materials. Another important feature of ILs is their nonvolatility, which facilitates recycling and containment. Cations and anions can be chosen to make ILs with low ecotoxicity and good biodegradability,

probably with a compromise in terms of the optimum functional properties for the intended process or device.

ILs can dissolve considerable amounts of cellulose, particularly 1-butyl-3-methylimidazolium chloride, [C₄C₁im]Cl, or 1-ethyl-3-methylimidazolium acetate, [C₂C₁im][OAc]. When precipitated with water, ethanol,⁴ or carbon dioxide,⁵ an amorphous cellulose structure is produced. This success led to further investigation of ILs to dissolve lignocellulosic materials.^{6–10} However, a detailed physicochemical understanding of the molecular mechanisms of dissolution is still lacking, and this fundamental knowledge is essential to design the best IL media to process cellulose.

Molecular simulation is a useful tool to build a microscopic view of the structure and dynamics of cellulose interacting with solvents. Atomistic models are detailed and represent well the entire set of relevant aspects: conformational flexibility of molecules or macromolecules, interaction potentials (electrostatic, H bonds, van der Waals), and the statistical thermodynamics of liquid phases in their configurational space. The literature contains some reports in which several kinds of molecular dynamics (MD) methods were used to investigate the dissolution of cellulose in ILs.

Received: August 11, 2014

Revised: November 26, 2014

Published: December 1, 2014



Singh and collaborators¹¹ at Sandia Laboratories followed the evolution of a bundle of nine cellulose chains of six glucans in $[C_2C_1im][OAc]$ by MD simulation for 100 ns. They studied conformations, H bonding, and chain mobility. They had previously studied by MD an isolated chain in three solvents: $[C_2C_1im][OAc]$, water, or methanol.¹² Cheng et al. of Oak Ridge reported MD simulations of a 36-chain cellulose microfibril in water and in $[C_4C_1im]Cl$ for 40 ns.¹³

Chu and his group at Berkeley published a series of papers between 2010 and 2012 on biomass recalcitrance to dissolution, looking at water and ILs as solvents.^{14–17} The model microfibril had 36 chains of 16 glucans, and initially a study of solvation in water was reported,¹⁴ followed by another including an all-atom model of $[C_4C_1im]Cl$.¹⁵ The deconstruction of a microfibril was studied by peeling apart one of the chains using potential of mean force methods, on a coarse-grain model of cellulose and of the IL.¹⁶ A further level of “coarse graining” was achieved through a lattice model¹⁷ used to simulate by Monte Carlo the effect of temperature on the structure of the fibril.

Rabideau and Ismail from Aachen recently reported MD studies of small bundles¹⁸ of cellulose and of a solvated chain¹⁹ in three imidazolium ILs having different anions and investigated the bundle breakup mechanism.

These studies contributed, in our opinion, to advance very significantly our knowledge about the processes involved in the dissolution of cellulose in ILs: while anions bind strongly to the hydroxyl groups of the exterior strands of the bundle, forming negatively charged complexes, cations intercalate between the individual strands, likely due to charge imbalances, pushing the chains apart and initiating their separation. However, they focused on pure ILs. An interesting feature of ILs that can be explored is their miscibility with molecular compounds, such as water or organic solvents. This miscibility can be tuned, for instance, by varying the length of alkyl side chains on the cation or through choice of anion. Water and alcohols are considered as antisolvents, with the role of precipitating cellulose out of the IL solution, regenerating a cellulosic material in a less recalcitrant form.²⁰ Here we focus rather on a molecular cosolvent.

The role of a cosolvent, in the present study dimethyl sulfoxide (DMSO), was analyzed from the perspective of its interactions with the IL and with the biopolymer and also in terms of its effect in lowering the viscosity of the medium, leading to accelerated dynamics and improved mass transport. The choice of DMSO was explained in a recent experimental study of solubility and dissolution kinetics of microcrystalline cellulose in mixed IL+DMSO solvents.²¹ DMSO is a polar (dipole moment of 4 D), nonprotic solvent and an acceptor of H bonds. It was found to be able to dissolve 10% w/w of cellulose at 373 K when only 0.1 mole fraction of $[C_2C_1im][OAc]$ was added.²²

The present study aims at elucidating the details of the interactions of DMSO and the IL $[C_4C_1im][OAc]$ with cellulose as well as of the onset of dissolution mechanism. We use MD simulation as “computer experiments” to follow the evolution of a model cellulose microfibril immersed both in the IL and in the IL+DMSO solvent systems using realistic molecular interaction and conformation models (force fields). Cellulose, the IL, and DMSO are represented at a fully atomistic level, allowing an observation of detailed conformational features and H bonding. This should help us understand important open questions about the keys to improve cellulose dissolution, for example, if it would be more promising to

proceed through increased energetics of interaction with the solvent or else through faster dynamics and transport in the medium.

COMPUTATIONAL METHODS

Cellulose consists of D-glucopyranose monomers (glucan units) connected by β -1,4 glycosidic linkages (Figure 1), forming relatively straight chains with degrees of polymerization from 100 to 20 000 monomer units. The chains form microfibrils. In this study, the model of a cellulose microfibril was constructed based on the crystal structures of I_β cellulose via the Cellulose-builder software.²³ The model microfibril contains 36 chains organized into 8 sheets (Figure 2), and each chain contains 10 glucan residues. Some simulations were performed on isolated, solvated oligosaccharide chains of two, four, and six glucan units (cellobiose, cellotetraose, and cellohexaose, respectively).

The force field used is a fully atomistic and flexible model for carbohydrates, OPLS-AA 2005,²⁴ which was shown to be among the best molecular force fields for oligosaccharides²⁵ and is compatible with widely used atomistic models for organic compounds and ILs. For the ions (Figure 3) a force field of the same type was used but with specific parameters for ILs.²⁶ DMSO was also represented by a compatible force field.²⁷

The starting configurations of the simulations were created using the Packmol software.²⁸ For the trajectories involving a microcrystal the system consists of an I_β microfibril centered in a cubic box containing 1500 $[C_4C_1im][OAc]$ ion pairs, giving a concentration of 16.6 wt % cellulose. The resulting length of cubic unit cell is \sim 80 Å with the total number atoms close to 55 700. An additional simulation was carried out with the microfibril in a mixed solvent composed of $[C_4C_1im][OAc]$ +DMSO (molar ratio 1:1) containing 1100 ion pairs and 1100 cosolvent molecules. The solvated chains were simulated with 300 ion pairs of IL.

Simulations were performed using the LAMMPS²⁹ MD software. The cutoff distance for nonbonded interactions was 12 Å. Long-range electrostatics were treated by the PPPM Ewald method. Bond distances involving hydrogen atoms were constrained using the SHAKE algorithm. Temperature and pressure (1 bar) were regulated by Nosé–Hoover thermostat and (isotropic) barostat with coupling time constants 100 and 1000 fs, respectively. The time step of the simulations is 1 fs. The isolated oligosaccharide chains in solution were simulated for 10 ns at 423 K after 200 ps of equilibration. (To overcome the slow kinetics of conformational changes and to attain better sampling, the simulations of the single chains were performed

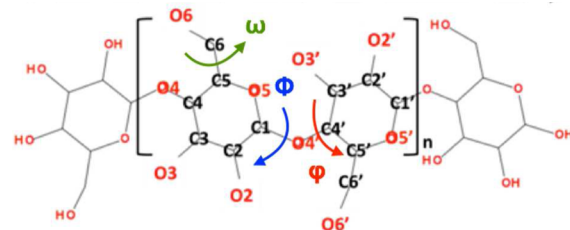


Figure 1. Molecular representation of the cellulose chain with atomic site labels on a cellobiose unit. In the present work we number glucan units or glycosidic linkages from the nonreducing end of the chain (left on the scheme) to the reducing end (right). Torsion angles are identified on the glycosidic linkage and on one $-\text{CH}_2-\text{OH}$ side group.

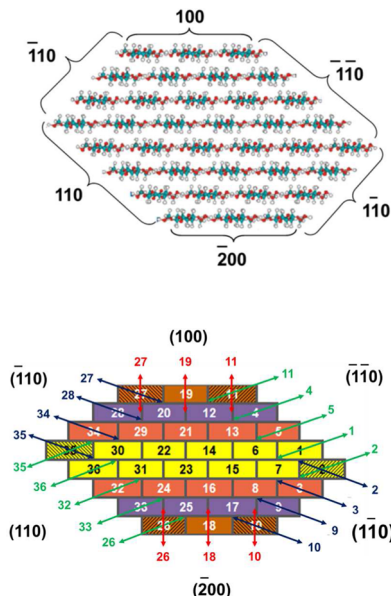


Figure 2. Cross-section and different surfaces of the model cellulose microfibril (top). Numbering convention identifying each chain (bottom). The surfaces (100) and $(\bar{2}00)$ are called hydrophobic, whereas the remainings are called hydrophilic surfaces.

at a higher temperature than the subsequent trajectories with a microcrystal.)

The initial configurations with microfibrils were allowed to relax with 100 ps zero-temperature minimizations, followed by preliminary NpT runs of 200 ps at 30 K, after which temperature was gradually increased to 300 K. Later, 500 ps at 300, 500, and 373 K NpT annealing runs were performed. With the cellulose fibril in $[C_4C_1im][OAc]$ + DMSO, a run of 2 ns at 300 K was performed for equilibration. Finally, a 3 ns run at 373 K was performed to equilibrate the system before statistics were collected. Trajectories of the equilibrated systems were generated at 373 K for 10 ns, with configurations saved every 1000 steps.

Such time scale is, of course, too short to observe the dissolution process of a cellulose microcrystal. However, it should provide a sufficiently long trajectory of the system for us to study the solvation of the microfibril and to observe the onset of dissolution. The detailed atomistic models will allow us to inspect conformational details and H bonding from such “computer experiments”.

RESULTS AND DISCUSSION

Simulations of the solvated oligosaccharide chains allow us to analyze the conformer distributions, in particular, the torsions around the glycosidic links as identified in Figure 1. The results for the five linkages in cellobiose are shown in Figure 4. It is seen that the glycosidic linkages adopt similar values for the two dihedral angles, which nonetheless span on the order of 150°.

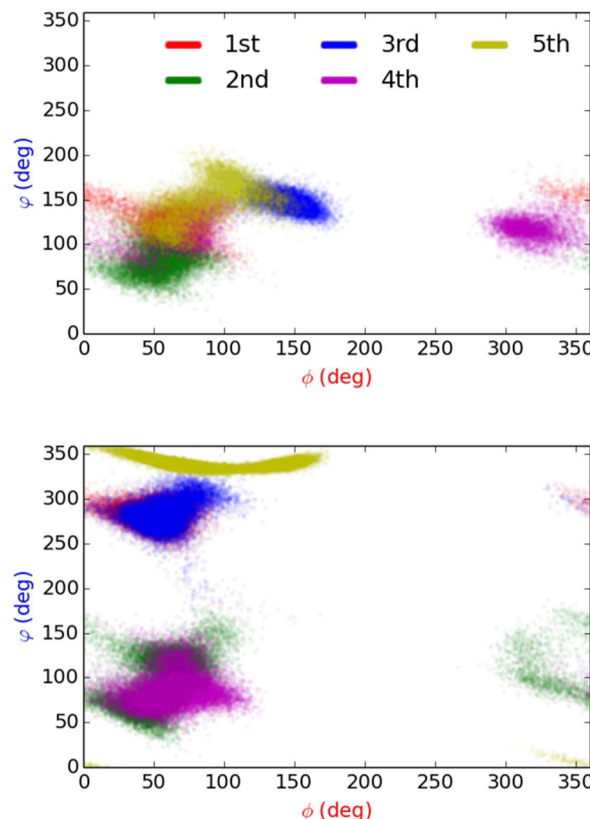


Figure 4. Distributions of the torsion angles involving the five glycosidic linkages of cellobiose at 423 K in the imidazolium acetate ionic liquid (top) and in the mixed solvent with DMSO (bottom).

The result is that the cellobiose chain remains mostly straight during the entire trajectory in $[C_4C_1im][OAc]$, as can be seen in a plot of the end-to-end distances of the oligosaccharides in Figure 5. The average end-to-end distance in pure IL is 28 Å with a standard deviation of 2 Å. The end-to-end distance fluctuations are mainly due to vibration modes without implying persistent conformational jumps. The visual inspection of the trajectory confirms that the chain is mostly linear. In addition, smaller chains with two and four glucans were also simulated in the pure IL (not reported in the manuscript), showing that the average end-to-end distance scales linearly with the number of glucan units. The persistence length of the cellulose polymer in the pure IL is thus greater than six monomers. In that sense, the chain was considered straight. Although the duration of the trajectory is too short to actually observe a sufficient number of conformational transitions to have meaningful statistics, the straight configuration suggests that the IL is a “good solvent” for the oligosaccharide.

The distribution of the torsional angle of $-\text{CH}_2-\text{OH}$ groups as a function of simulation time is shown in Figure 6, where fast

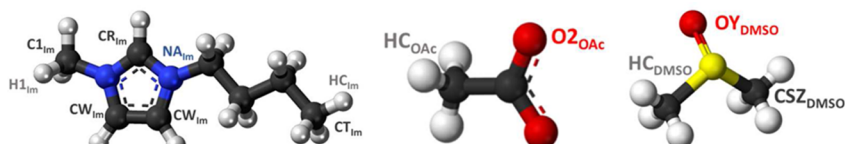


Figure 3. Atom labeling of 1-butyl-3-methylimidazolium cation, acetate anion and dimethyl sulfoxide.

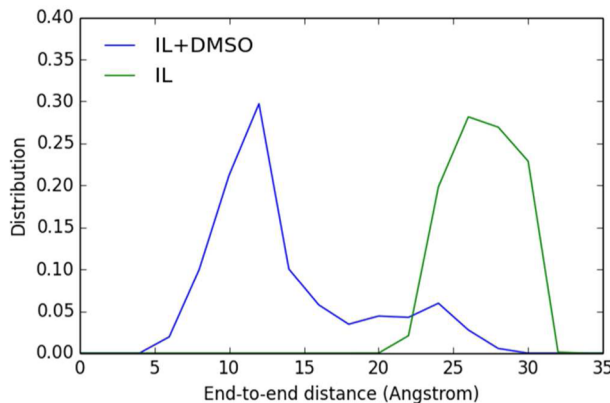


Figure 5. Distribution of the end-to-end distance of the cellohexaose chain in the imidazolium acetate ionic liquid and in its mixture with DMSO.

interconversion between three conformers is seen within the duration of the trajectory.

A single cellohexaose molecule was then simulated in a mixture of DMSO and [C4C1im][OAc]. A visual inspection of the trajectory reveals that the cellohexaose chain is not straight anymore. The histogram of the end-to-end distance (Figure 5) shows that the chain is indeed folded. This means that the solvent containing DMSO is not as good as the pure IL. The difference in conformation is also apparent in the dihedral distribution of the glycosidic linkages seen in Figure 4.

Although DMSO has a strong electric dipole, it forms very few H bonds with the OH groups of the cellohexaose (Table 1). H bonds X-H \cdots Y are defined here using a geometrical criterion: the H \cdots Y distance must be $<3.2\text{ \AA}$ and the X-H \cdots Y angle must be $>130^\circ$. Most H bonds link cellohexaose OH to acetate oxygens. All OH groups have similar tendency to form H bonds except for the freer O6-H of the hydroxymethyls, which form more H bonds intrachain or toward DMSO. The intrachain H bonds are, in particular, present between neighboring glucans (mostly O6-H \cdots O3), in which case they seem to form cooperatively: when two consecutive glucans are linked by a H bond, they are more frequently linked by a second H bond. This cooperation must contribute to the chain rigidity. Fewer intrachain H bonds also occur intraglucan (mostly O6-H \cdots O5) or between nonconsecutive glucans, which helps the chain folding.

During this simulation, many intrachain H bonds formed between the glucans 5 and 6, along the fifth glycosidic linkage.

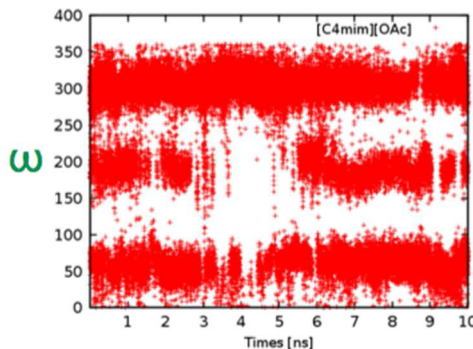


Figure 6. Values of the torsion angle of the $-\text{CH}_2\text{-OH}$ groups in cellohexaose plotted as a function of the simulation time.

Table 1. Average Number of H Bonds Per Donor for the Cellobetaose in The DMSO-[C4C1im][OAc] Mixture ($\times 1000$)

	O3-H	O2-H	O6-H	O4-H end	O1-H end
O2OAc	1190.37	1296.49	850.88	1223.54	1200.24
O3	0.00	3.33	106.56	1.80	0.00
O2	7.82	3.62	17.17	0.00	4.10
O5	40.40	0.22	13.67	0.00	0.00
OYDMSO	8.52	3.02	36.66	7.15	10.70
total	1247.11	1306.68	1024.94	1232.49	1215.04

This constrained the changes in conformation and can explain why the distribution of torsion angles of the fifth glycosidic linkage is so narrow in Figure 4.

The conformational mobility of cellulose chains in the microfibril was assessed by calculating the mean-squared displacement of each glucan unit during the MD trajectory. The torsional angles considered are those of Figure 1. Figure 7 shows the distribution of dihedrals of the nine glycosidic linkages (counting from the nonreducing end) averaged over all chains. It can be seen that the terminal linkages (1 and 9) have distributions that span a broad range of angles, whereas the inner dihedrals stay more rigid around ca. 270° , which may be the indication of lack of ions diffusing to the groups in between 1 and 9 during the simulation time. The cellulose chain has a polarity that arises from the chemical difference of the two ends. Because of the chemical differences of reducing and nonreducing ends, there are different dihedral angle distributions and density profiles of solvents around these end groups when the cellulose fibrils are solvated in ILs. In the presence of DMSO, the histograms of the terminal linkages are smoother (Figure 7), meaning that conformations are better equilibrated

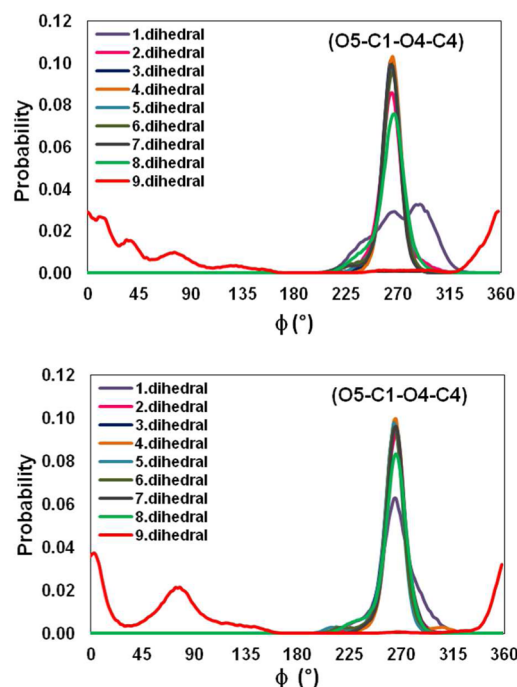


Figure 7. Distribution of dihedral angles Φ (O5-C1-O4'-C4') of the glycosidic linkages for the fibril in IL (top) and in IL+DMSO (bottom), averaged over all chains of the microfibril. Equivalent results for φ (C5'-C4'-O4'-C1) are given in Figure S1 of the Supporting Information.

on the time scale of the simulation when compared with the situation in pure IL.

We observe that the distribution of dihedral angles numbered 1 (near the nonreducing end) is broader but “noisier” with multiple small peaks in the pure IL compared with when DMSO is present, in which case one smooth, high peak is observed. Dihedrals numbered 9 (near the reducing end) also show many small peaks in pure IL and only two well-defined ones in IL+DMSO. During the trajectory in the pure IL (more viscous solvent) the torsions are stuck in certain conformations and do not show smooth histograms around the prominent energy minima, whereas in IL+DMSO the fluidity of the solvent allows for a better equilibration of the conformations. There is a marked difference between the conformations adopted by the two ends of the fibril. On the nonreducing end the dihedrals 1 show a distribution quite similar to those of the inner dihedrals of the chain (2 to 8), all with single-peaked distributions around 270°. On the reducing end, in contrast, dihedrals 9 show a totally different distribution around the two most likely angles at 360 and 80°. Solvation and destructuring of the fibril by the medium therefore seems more pronounced at the reducing end.

In Figure 8 histograms of dihedral angle corresponding to the rotation of the hydroxymethyl groups are shown, in IL and in IL+DMSO. In both solvents a 3-modal distribution occurs, with more evenly distributed populations in the mixed solvent. The hydroxymethyl groups of the microfibril that are exposed to the solvent play an important role in the interactions with the medium. These groups can rotate around the C5–C6 bond to adopt three conformations according to the trans and gauche position of each dihedral (Figure S6 in the Supporting Information). In the simulations of Liu et al.¹¹ the distribution in the I_B crystal is tg > gt > gg, in agreement with the experiments of Langan et al.³⁰ However, their model cellulose

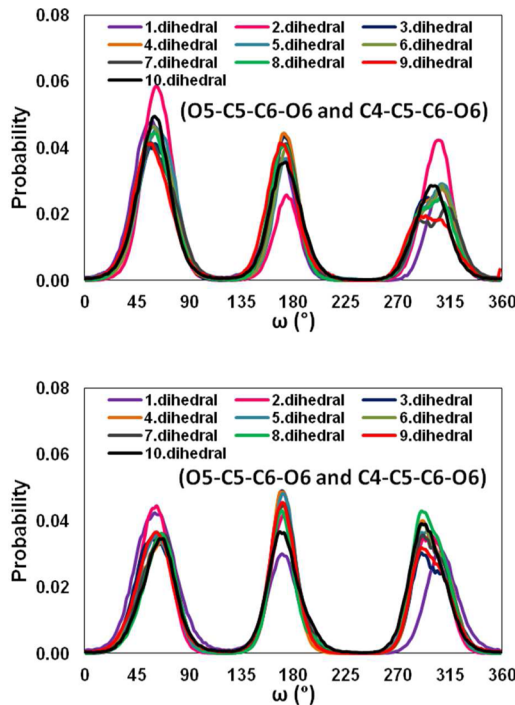


Figure 8. Distributions of dihedral angles ω of the hydroxymethyl side groups of the glucan units in IL (top) and IL+DMSO (bottom), averaged over all chains in the microfibril.

in [C₂C₁im][OAc] shows a very different distribution of torsion angles, with a majority of gt, some gg conformations, and the tg at <1%.¹¹ A preference for the gg conformation, followed by the gt conformation, was found by other computational studies in aqueous solution.³¹ Our results agree with this general picture of preferred gg and gt conformations. More detailed plots of distributions of the three dihedral angles studied, but concerning the chains on each exposed surface of the microfibril, are given in the Supporting Information (Figures S1–S8).

The mobility of the chains was assessed through the root-mean-squared displacement (RMSD) of the atoms in the cellulose microcrystal, averaged for each chain over the length of the MD trajectory. The results are shown in Figure 9, both in IL and in IL+DMSO. It can be seen that certain chains have higher mobility, namely, those more exposed to the solvent (cf. Figure 2), for instance, chains 27, 2, 10, or 35. Mobility is highest for chains on the edges and on the (1̄10) and (110̄) surfaces. These chains are more mobile than those on the other two hydrophilic surfaces, (110) and (100̄). The rmsd's are systematically higher in the mixed IL+DMSO solvent when compared with those in pure IL.

The slight increase in the intersheet distance is likely caused by the insertion of ions from the IL, leading to an expansion of the cellulose lattice. Experimental evidence of this swelling was reported recently^{10,32} revealing a 6% expansion of the intersheet distance. To see the swelling or opening of the end-groups of chains, we measured the distance between oxygen atoms (O5) of glucose rings in the extremities and center of the chains, as shown in Figure 10. In the presence of

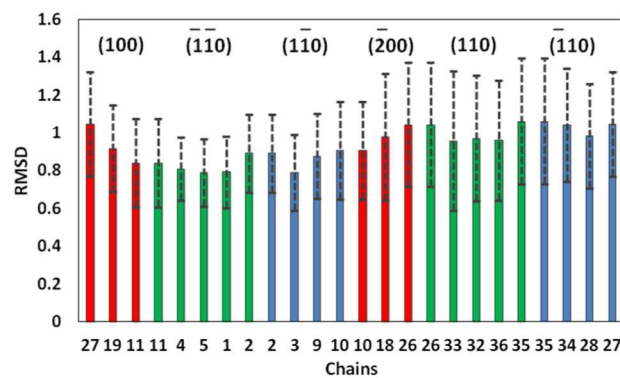
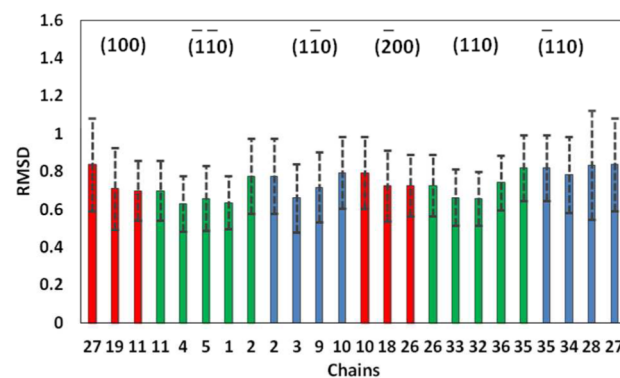


Figure 9. Chain mobility evaluated through the root-mean-squared displacements of atoms in each chain of the fibril in IL (top) and in IL+DMSO (bottom).

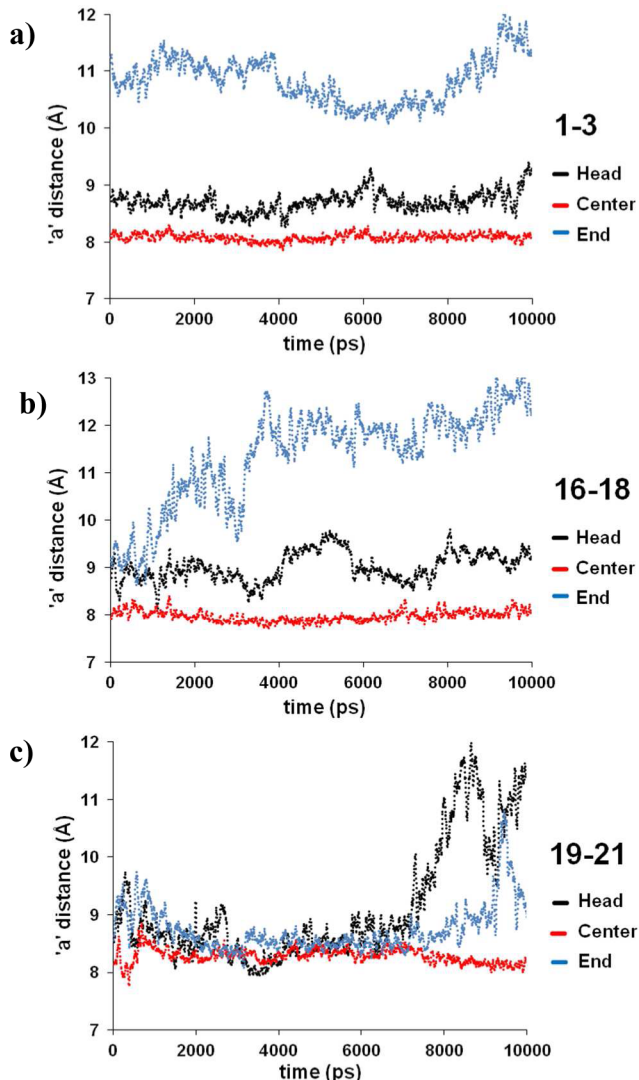


Figure 10. Plots of the distance ' a' ' between oxygen atoms (O_5) of glucose units from the tail (nonreducing end), head (reducing end), and the center of cellulose chains. The upper plot corresponds to pure IL (a), and the bottom corresponds to two to IL+DMSO (b,c). The examples chosen are those where larger displacements were observed in the two solvents or an interesting "event" during the course of the trajectory. Further examples are given in the Supporting Information (Figures S9 and S10).

DMSO swelling appears to occur more easily at the middle chains of the hydrophobic surfaces (e.g., chains 16, 18 on one side and 19, 21 on the other). Interestingly, sometimes it is the nonreducing end that shows higher distances, meaning that although this end of the chains is less affected in terms of conformational changes (see Figure 7), it can show translational mobility on a par with the reducing end.

Hydrogen bonding is dominant in solvation and in the cohesion of cellulose particles. Cellulose fibrils contain intrachain, interchain, and intersheet H bonds as illustrated in Figure 11. In the present simulations an H bond is defined based on the crystal structures of carbohydrates^{14,33} by the following geometric criteria: (i) the distance between the donor and acceptor oxygen atoms must be less than 3.2 Å and the angle of $O-H\cdots O$ must be greater than 130° and (ii) the distance between the donor carbon and acceptor oxygen atoms

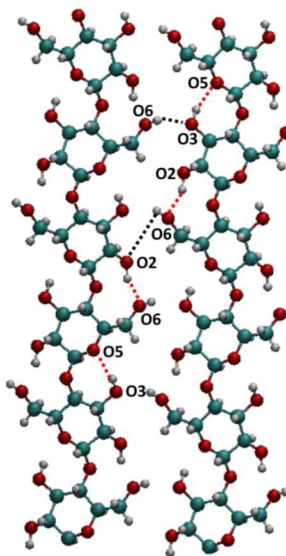


Figure 11. Main H-bonding pattern in cellulose.³⁰ Intrachain hydrogen bonds ($O_3-H\cdots O_5$ and $O_2-H\cdots O_6$) are indicated by green dots. Interchain hydrogen bonds ($O_6-H\cdots O_3$ and $O_6-H\cdots O_2$) are indicated by black dots. Numerous C-H...O contacts and van der Waals interactions connect chains on neighboring sheets (intersheet).

must be <4.2 Å and the angle of $C-H\cdots O$ must be $>110^\circ$. The specific H bonds are identified in Table 2.

Statistics on the three types of hydrogen bond were calculated and are presented in Figure 12. Combining all three types, the average number of H bonds per glucose residue is shown in Figure 12d. The total number of H bonds per glucose is higher in the interior and decreases toward the surface due to a lack of bonding partners. The chains on the two hydrophobic surfaces have fewer hydrogen bonds, which decrease gradually from top to bottom. It can be concluded that the intersheet H bonds are the main cause of stabilization of the cellulose structure.

Hydrogen-bond statistics between the exposed cellulose chains and the solvent are shown in Figure 13. The predominant H bonds are those in which cellulose OH groups act as donors toward the O atoms of the acetate anions. Although, to a smaller extent, cellulose also interacts with the cations as H bond acceptor, with the H atoms of the imidazolium ring of the cations interacting with the O atoms of the polysaccharide ($C_{R,W}-H\cdots O$, involving the aromatic C atoms of the imidazolium ring). The chains that showed greater mobility and swelling effect are those that are more exposed

Table 2. Identification of the Intrachain, Interchain, and Intersheet Hydrogen Bonds That Exist in the Crystal Structure

type	interaction (D-H \cdots A)	type	interaction (D-H \cdots A)
intrachain	$O_3-H\cdots O_5$	intersheet	$C_2-H\cdots O_6$
intrachain	$O_2-H\cdots O_6$	intersheet	$C_4-H\cdots O_2$
interchain	$O_6-H\cdots O_2$	intersheet	$C_3-H\cdots O_2$
interchain	$O_6-H\cdots O_3$	intersheet	$C_3-H\cdots O_6$
intersheet	$C_1-H\cdots O_3$	intersheet	$C_5-H\cdots O_3$
intersheet	$C_1-H\cdots O_6$	intersheet	$C_5-H\cdots O_4$
intersheet	$C_2-H\cdots O_3$	intersheet	$C_6-H\cdots O_2$
intersheet	$C_2-H\cdots O_4$	intersheet	$C_6-H\cdots O_5$

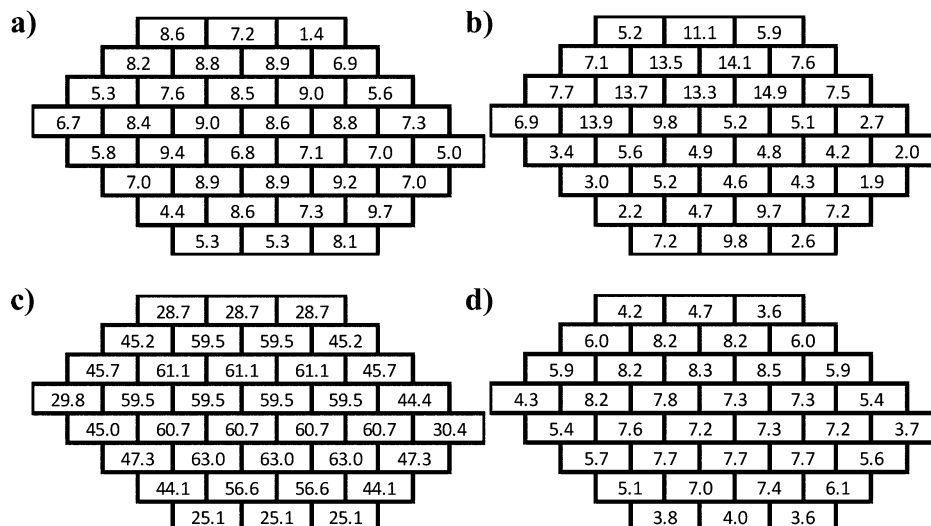


Figure 12. Number of hydrogen bonds in the microcrystal (in pure IL) per chain: (a) intrachain, (b) interchain, (c) intersheet, and (d) total per chain and per glucose unit. Results averaged over 10 ns.

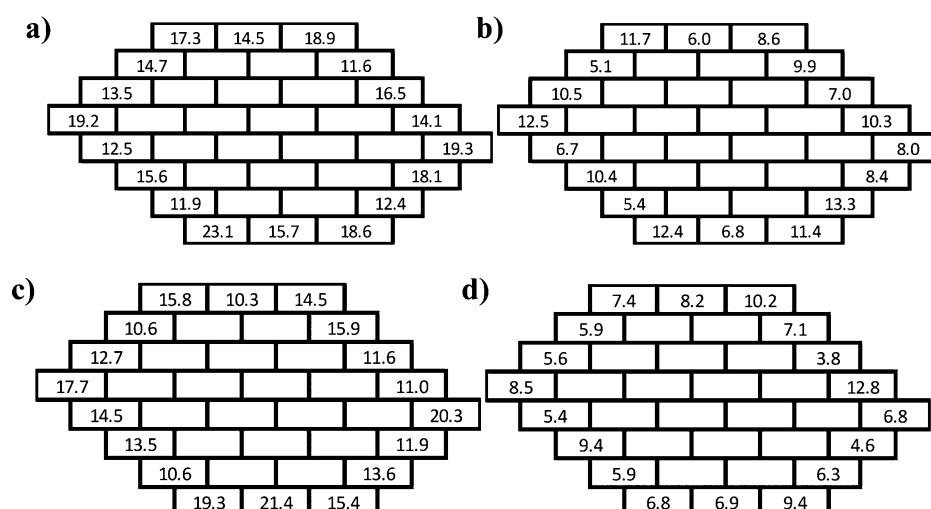


Figure 13. H bonds between the exposed chains of the microfibril and the solvent. Left (a,c): between hydroxyl groups of cellulose and oxygen atoms of the acetate anions. Right (b,d): between H atoms bonded to aromatic C atoms (CR and CW) of the imidazolium ring and O atoms of cellulose. Top (a,b): in pure IL. Bottom (c,d): in IL+DMSO. Results per chain averaged over 10 ns.

and that H-bond more strongly with the solvent (chain 26 participates in many H bonds with both cations and anions).

A comparison of the number of H bonds between cellulose and the ions in pure IL and in IL+DMSO (mole fraction 0.5) shows a decrease in the latter case. However, this decrease is small, taking into account the dilution factor of the IL. This observation reinforces the view that DMSO does not interfere strongly with the interactions between the IL and cellulose.

A better understanding of the local solvation environments involving the imidazolium and acetate ions and DMSO can be obtained from the radial distribution functions (RDFs) in the solvent. The RDF $g(r)$ gives the probability of finding a given pair of atomic sites at a certain mutual distance compared with the average probability. Some chosen RDFs are shown in Figure 14 to illustrate the liquid-phase structure. Intense first peaks are obtained between the O atoms of acetate anions (sites of negative partial charge) and H_{CR} or H_{CW} atoms of the imidazolium rings of the cations. Contrasting with these strong cation-anion interactions, first peaks involving DMSO are much less intense. Also, the RDF between DMSO oxygen and

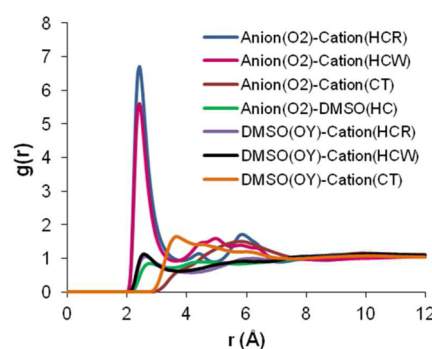


Figure 14. Selected site-site radial distribution functions involving: oxygen atoms of anion (O_2), oxygen atoms of DMSO (OY), hydrogen atoms (H_{CR} , HCW) of the imidazolium ring of the cation, the terminal carbon atom (CT) of the alkyl side chain of the cation, and hydrogen atoms of DMSO (HC).

the end-carbon of the alkyl side chain shows a slightly intense first peak. These two features mean that positional correlations

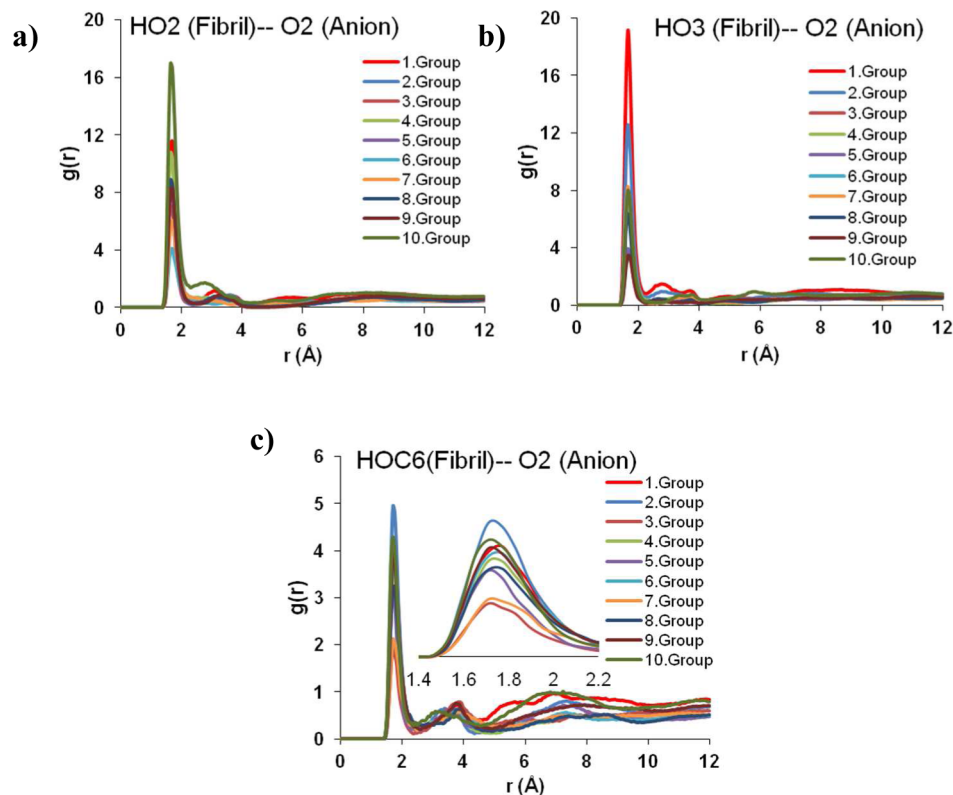


Figure 15. Site–site radial distribution functions involving OH groups (HO2 (a), HO3 (b) and HOC6 (c)) of cellulose and oxygen atoms of anion (O_2) per glucan residue along the microfibril in IL+DMSO.

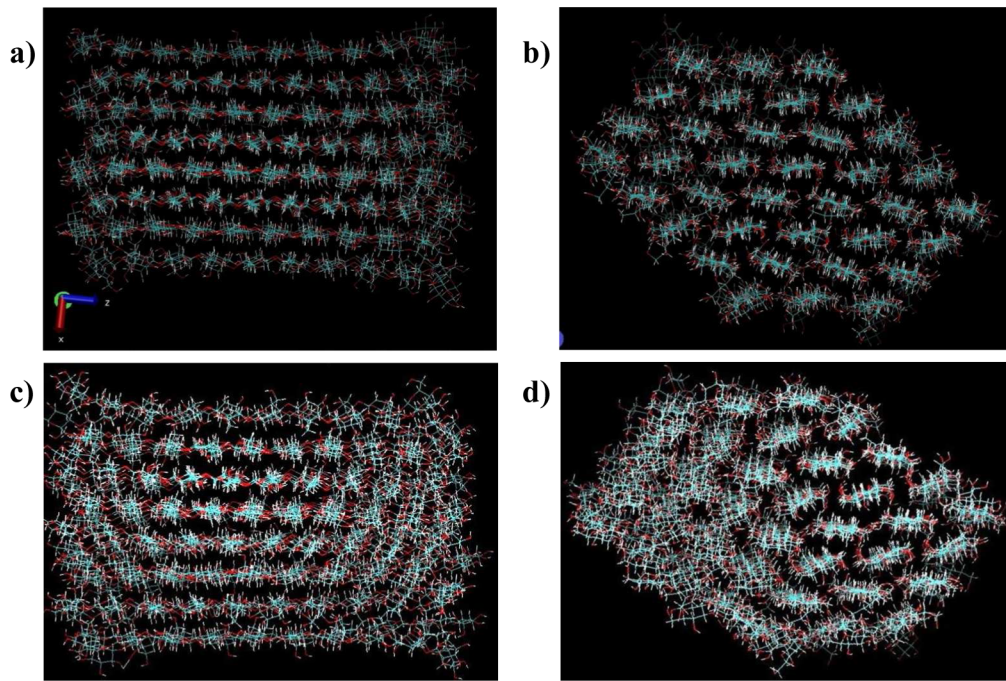


Figure 16. Snapshots of the final state of the microfibril after the 10 ns trajectory. Top: views along (a) and across (b) the polymerization axis in pure IL. Bottom: views along (c) and across (d) the polymerization axis in IL+DMSO.

of DMSO with the electrostatically charged parts of both cations and anions are rather weak despite the high dipole moment of DMSO.

RDFs between OH groups of cellulose, namely, those in positions 2 and 3 (see Figure 11), and the oxygen atoms of the

acetate anion are shown in Figure 15 in the mixed solvent IL +DMSO. It is seen that the OH groups in position 2 of the glucans form H bonds, with acetate mainly at the reducing end (glucan numbered 10), whereas the OH groups in position 3 of the glucans form H bonds with acetate mainly in the

nonreducing end (glucan number 1). OH groups in position 6 of the glucans form more H bonds with acetate in the middle of the chains. These are logic results, corresponding to the highest accessibilities to the solvent. The results are very similar in the pure IL (shown in Figure S11 in the Supporting Information), meaning that DMSO does not disrupt to a large extent the H bonds between cellulose and the IL. In fact, DMSO interacts slightly more with the OH group in position 3, although with a very weak intensity when compared with those with acetate. This can be seen in Figure S12 of the Supporting Information. Additional, more detailed examples of RDFs are shown in Figures S13–S16 of the Supporting Information, which contain several RDFs calculated per glucan monomer, per exposed chain, and per surface of the microfibril.

The final state of the microfibril after the 10 ns MD trajectory, in both pure $[C_4C_1im][OAc]$ and in this IL mixed with DMSO, can be seen in Figure 16. The local densities of ions and of DMSO, which are complementary pictures from the one in Figure 16, can be seen in Figures S17 and S18 of the Supporting Information, which represent the density profile of anion, cation, and DMSO along each surface of the fibril. The distance between DMSO and cellulose chains is comparable to that of cations but smaller than the distance between anions and the cellulose fibril. Although some deconstruction of the exposed chains and of the terminal glucans is already apparent in the fibril solvated by pure IL, a much more important loss of crystalline structure is evident in the fibril solvated in IL +DMSO.

CONCLUSIONS

The results of MD trajectories reported here of a cellulose microfibril solvated in both pure $[C_4C_1im][OAc]$ and in an equimolar mixture of this IL+DMSO all lead to a coherent picture of the role of the molecular cosolvent in the dissolution of cellulose. Despite its high dipole moment and accessible oxygen atom, DMSO does not establish specific associating interactions with cellulose or with the ions: DMSO is not able to significantly disrupt H bonds between cellulose and the ions (mostly the anion), and neither is able to disrupt cation–anion close contacts to a relevant extent.

In this work we used detailed, fully atomistic models both for the cellulose microfibril and for the IL. Although the duration of the trajectories generated is much too short to attain dissolution and effectively only allows us to view the onset of the dissolution process, the level of detail it provides is useful to analyze effects on conformations, interactions (hydrogen bonding is of primary interest here), dynamics, and the nature of local solvation environments.

The results of the present simulations corroborate the findings of a recent experimental study:²¹ DMSO has the role of an “innocent” cosolvent, which does not interact strongly with cellulose, does not interfere with the interactions of cellulose with the IL, but lowers the viscosity of the medium, leading to faster mass transport and dissolution. The present molecular simulations provide insight into this qualification of “innocent” solvent, which concerns direct solvation interactions, although some DMSO molecules can be found near the fibril or even in interstitial zones. The spatial distributions of cations and anions with respect to the fibril found in pure IL are maintained when DMSO is present.

This role of the cosolvent in lowering the viscosity and improving mass transport is an important design concept for ionic solvent systems, allowing us to overcome one of the main

drawbacks of ILs, which is their high viscosity. Particularly in applications related to the dissolution of polymer materials, this limitation can quickly become severe. Increasing temperature can be a means of lowering viscosity, but this can have undesirable consequences in terms of energy consumption or thermal degradation. Adding a well-chosen cosolvent can be an interesting solution.

In this study DMSO was chosen for a number of reasons. (It had been identified as a good cosolvent for the dissolution of cellulose and is a polar, nonprotic compound.) We intend to pursue research on other, more environmentally friendly and efficient compounds, keeping the same principle of an “innocent” cosolvent of low volatility that fluidifies the ionic medium.

ASSOCIATED CONTENT

Supporting Information

Figures and plots of additional and more detailed results obtained from the MD trajectories on conformational aspects, hydrogen bonding, and RDFs. This material is available free of charge via the Internet at <http://pubs.acs.org>.

AUTHOR INFORMATION

Corresponding Author

*E-mail: agilio.padua@univ-bpclermont.fr.

Notes

The authors declare no competing financial interest.

ACKNOWLEDGMENTS

This work was supported by the Contrat d'Objectifs Partagés Thermodynamique Moléculaire (CNRS, Université Blaise Pascal, Conseil Régional d'Auvergne). One of authors was acknowledged by the Scientific and Technological Research Council of Turkey (TUBITAK) through the scholarship of international doctoral research fellowship program.

REFERENCES

- (1) Klemm, D.; Heublein, B.; Fink, H.-P.; Bohn, A. Cellulose: Fascinating Biopolymer and Sustainable Raw Material. *Angew. Chem. Int. Ed.* **2005**, *44*, 3358–3393.
- (2) Liebert, T. Cellulose Solvents – Remarkable History, Bright Future. In *ACS Symposium Series Cellulose Solvents: For Analysis, Shaping and Chemical Modification*; American Chemical Society; Liebert, T. F., Heinze, T. J., Edgar, K. J., Eds.; American Chemical Society: Washington, DC, 2010; Vol. 1033, pp 3–54.
- (3) Wasserscheid, P.; Welton, T. *Ionic Liquids in Synthesis*; Wasserscheid, P., Welton, Y., Eds.; 2nd ed.; Wiley-VCH: Weinheim, Germany; pp 1–740.
- (4) Swatloski, R.; Spear, S.; Holbrey, J.; Rogers, R. Dissolution of Cellulose with Ionic Liquids. *J. Am. Chem. Soc.* **2002**, *124*, 4974–4975.
- (5) Barber, P. S.; Griggs, C. S.; Gurau, G.; Liu, Z.; Li, S.; Li, Z.; Lu, X.; Zhang, S.; Rogers, R. D. Coagulation of Chitin and Cellulose From 1-Ethyl-3-Methylimidazolium Acetate Ionic-Liquid Solutions Using Carbon Dioxide. *Angew. Chem. Int. Ed.* **2013**, *52*, 12350–12353.
- (6) Pinkert, A.; Marsh, K. N.; Pang, S.; Staiger, M. P. Ionic Liquids and Their Interaction with Cellulose. *Chem. Rev.* **2009**, *109*, 6712–6728.
- (7) Heinze, T.; Dorn, S.; Schöbitz, M.; Liebert, T.; Köhler, S.; Meistner, F. Interaction of Ionic Liquids with Polysaccharides-2: Cellulose. *Macromol. Symp.* **2008**, *262*, 8–22.
- (8) Fukaya, Y.; Hayashi, K.; Wada, M.; Ohno, H. Cellulose Dissolution with Polar Ionic Liquids Under Mild Conditions: Required Factors for Anions. *Green Chem.* **2008**, *10*, 44–46.
- (9) Remsing, R.; Swatloski, R.; Rogers, R.; Moyna, G. Mechanism of Cellulose Dissolution in the Ionic Liquid 1-N-Butyl-3-Methylimid-

- zolum Chloride: a C-13 and Cl-35/37 NMR Relaxation Study on Model Systems. *Chem. Commun.* **2006**, 1271–1273.
- (10) Cheng, G.; Varanasi, P.; Arora, R.; Stavila, V.; Simmons, B. A.; Kent, M. S.; Singh, S. Impact of Ionic Liquid Pretreatment Conditions on Cellulose Crystalline Structure Using 1-Ethyl-3-Methylimidazolium Acetate. *J. Phys. Chem. B* **2012**, *116*, 10049–10054.
- (11) Liu, H.; Cheng, G.; Kent, M.; Stavila, V.; Simmons, B. A.; Sale, K. L.; Singh, S. Simulations Reveal Conformational Changes of Methylhydroxyl Groups During Dissolution of Cellulose I(B) in Ionic Liquid 1-Ethyl-3-Methylimidazolium Acetate. *J. Phys. Chem. B* **2012**, *116*, 8131–8138.
- (12) Singh, R.; Monk, J.; Hung, F. R. A Computational Study of the Behavior of the Ionic Liquid [BMIM+][PF₆-] Confined Inside Multiwalled Carbon Nanotubes. *J. Phys. Chem. C* **2010**, *114*, 15478–15485.
- (13) Mostofian, B.; Smith, J. C.; Cheng, X. The Solvation Structures of Cellulose Microfibril in Ionic Liquids. *Interdiscip. Sci.: Comput. Life Sci.* **2011**, *3*, 308–320.
- (14) Gross, A. S.; Chu, J.-W. On the Molecular Origins of Biomass Recalcitrance: the Interaction Network and Solvation Structures of Cellulose Microfibrils. *J. Phys. Chem. B* **2010**, *114*, 13333–13341.
- (15) Gross, A. S.; Bell, A. T.; Chu, J.-W. Thermodynamics of Cellulose Solvation in Water and the Ionic Liquid 1-Butyl-3-Methylimidazolium Chloride. *J. Phys. Chem. B* **2011**, *115*, 13433–13440.
- (16) Cho, H. M.; Gross, A. S.; Chu, J.-W. Dissecting Force Interactions in Cellulose Deconstruction Reveals the Required Solvent Versatility for Overcoming Biomass Recalcitrance. *J. Am. Chem. Soc.* **2011**, *133*, 14033–14041.
- (17) Chang, R.; Gross, A. S.; Chu, J.-W. Degree of Polymerization of Glucan Chains Shapes the Structure Fluctuations and Melting Thermodynamics of a Cellulose Microfibril. *J. Phys. Chem. B* **2012**, *116*, 8074–8083.
- (18) Rabideau, B. D.; Agarwal, A.; Ismail, A. E. Observed Mechanism for the Breakup of Small Bundles of Cellulose I α and I β in Ionic Liquids From Molecular Dynamics Simulations. *J. Phys. Chem. B* **2013**, *117*, 3469–3479.
- (19) Rabideau, B. D.; Agarwal, A.; Ismail, A. E. The role of the Cation in the Solvation of Cellulose by Imidazolium-Based Ionic Liquids. *J. Phys. Chem. B* **2014**, *118*, 1621–1629.
- (20) Singh, S.; Simmons, B. A.; Vogel, K. P. Visualization of Biomass Solubilization and Cellulose Regeneration During Ionic Liquid Pretreatment of Switchgrass. *Biotechnol. Bioeng.* **2009**, *104*, 68–75.
- (21) Andanson, J. M.; Bordes, E.; Devémy, J.; Leroux, F.; Pádua, A. H.; Costa Gomes, M. F. Understanding the Role of Co-Solvents in the Dissolution of Cellulose in Ionic Liquids. *Green Chem.* **2014**, *16*, 2528–2538.
- (22) Rinaldi, R. Instantaneous Dissolution of Cellulose in Organic Electrolyte Solutions. *Chem. Commun.* **2010**, *47*, 511–513.
- (23) Gomes, T. C. F.; Skaf, M. S. Cellulose-Builder: a Toolkit for Building Crystalline Structures of Cellulose. *J. Comput. Chem.* **2012**, *33*, 1338–1346.
- (24) Kaminski, G. A.; Friesner, R. A.; Tirado-Rives, J.; Jorgensen, W. L. Evaluation and Reparametrization of the OPLS-AA Force Field for Proteins via Comparison with Accurate Quantum Chemical Calculations on Peptides. *J. Phys. Chem. B* **2001**, *105*, 6474–6487.
- (25) Stortz, C. A.; Johnson, G. P.; French, A. D.; Csonka, G. I. Comparison of Different Force Fields for the Study of Disaccharides. *Carbohydr. Res.* **2009**, *344*, 2217–2228.
- (26) Canongia Lopes, J. N.; Deschamps, J.; Padua, A. A. H. Modeling Ionic Liquids Using a Systematic All-Atom Force Field. *J. Phys. Chem. B* **2004**, *108*, 2038–2047.
- (27) Bordat, P.; Sacristan, J.; Reith, D.; Girard, S.; Glättli, A. An Improved Dimethyl Sulfoxide Force Field for Molecular Dynamics Simulations. *Chem. Phys. Lett.* **2003**, *374*, 201–205.
- (28) Martínez, L.; Andrade, R.; Birgin, E. G.; Martínez, J. M. PACKMOL: a Package for Building Initial Configurations for Molecular Dynamics Simulations. *J. Comput. Chem.* **2009**, *30*, 2157–2164.
- (29) Plimpton, S. J. Fast Parallel Algorithms for Short-Range Molecular Dynamics. *J. Comput. Phys.* **1995**, *117*, 1–19.
- (30) Nishiyama, Y.; Langan, P.; Chanzy, H. Crystal Structure and Hydrogen-Bonding System in Cellulose I β From Synchrotron X-Ray and Neutron Fiber Diffraction. *J. Am. Chem. Soc.* **2002**, *124*, 9074–9082.
- (31) Shen, T.; Langan, P.; French, A. D.; Johnson, G. P.; Gnanakaran, S. Conformational Flexibility of Soluble Cellulose Oligomers: Chain Length and Temperature Dependence. *J. Am. Chem. Soc.* **2009**, *131*, 14786–14794.
- (32) Wada, M.; Kondo, T.; Okano, T. Thermally Induced Crystal Transformation From Cellulose I α and I β . *Polym. J.* **2003**, *35*, 155–159.
- (33) Steiner, T.; Saenger, W. Geometry of C-H···O Hydrogen Bonds in Carbohydrate Crystal Structures: Analysis of Neutron Diffraction Data. *J. Am. Chem. Soc.* **1992**, *114*, 10146–10154.